JOURNAL OF CATALYSIS **158,** 267–278 (1996)
ARTICLE NO. 0026

Coke Formation and Its Effect on Internal Mass Transfer and Selectivity in Pd-Catalysed Acetylene Hydrogenation

Staffan Asplund

Department of Chemical Reaction Engineering, Chalmers University of Technology, S-412 96 Gothenburg, Sweden

Received May 19, 1995; revised September 13, 1995

Catalyst aging by coke formation has been studied for the selective hydrogenation of acetylene in the presence of excess ethylene on supported palladium catalysts. Deposited coke was found to have a substantial influence on the effective diffusivity, which decreased about one order of magnitude during 100 h of operation. As has been observed previously the selectivity for the undesired ethane was higher on aged catalysts, while the activity for acetylene hydrogenation was almost constant. These effects, however, were strongly dependent on the catalyst particle size, although the behaviour of fresh catalysts was unaffected by mass transfer limitations. When the catalyst used was Pd/α-Al_2O_3 the change in selectivity with aging could be explained solely as a consequence of the increased diffusion resistance. The mass transfer effects were important also on Pd/γ-Al_2O_3, but on this catalyst there was an additional increase in ethane selectivity that could not be attributed to diffusion limitations. Calculations and experimental tests showed that the observed phenomena are relevant also for the shell-type catalysts normally used industrially. The coke formation itself was about four to five times faster on Pd/γ-Al_2O_3 compared to the α-Al_2O_3-supported catalyst. The coke was generally concentrated towards the pellet periphery showing the influence of diffusion resistance also on the coke-forming reactions.

INTRODUCTION

The selective hydrogenation of acetylene in ethylene is a commercially important process used to remove trace amounts of acetylene from polymer-grade ethylene streams. A very high selectivity is required as the acetylene content must be reduced to a few parts per million without any significant ethylene hydrogenation. An additional difficulty is that the ethylene to acetylene ratio in the feed can be as high as 100. The industrial processes normally use supported palladium catalysts with carbon monoxide added to the feed as a selectivity promoter. A survey of commercial processes can be found in (1).

This reaction system is also interesting from a scientific point of view and has received considerable attention in the literature. The work on kinetics and mechanisms has recently been reviewed by Bos and Westerterp (2). The crucial role of carbon monoxide as a selectivity promoter has been studied by many investigators (3–5). It is noteworthy however that in spite of the amount of published work, very few rate equations are found in the literature. According to Bos and Westerterp (2) this is probably due to the very complex nature of this system.

In addition to the intriguing kinetics the system also shows unusual aging behaviour. It is well known that acetylene is not only hydrogenated, but also undergoes hydropolymerisation reactions. These lead primarily to various C_4 compounds but also to higher hydrocarbons (oligomers), most of which are retained on the catalyst. The retained fraction can under some conditions eventually form a liquid phase, often referred to as ''green oil.'' The accumulation of hydrocarbon residues on the catalyst surface leads to interesting deactivation phenomena, which have been studied by several groups (6–8). The traditional gas-phase process has been compared to the novel liquid-phase process with respect to deactivation by Asplund *et al.* (9). In the absence of carbon monoxide the activity for acetylene hydrogenation is often observed to remain constant with time on stream while the selectivity is dramatically affected. Sárkány *et al.* (6) studied deactivation at low acetylene concentration (0.05–0.1%) and atmospheric pressure. They found that the ethylene hydrogenation rate increased largely during the first 100 h of operation on catalysts with a high area support (λ-Al_2O_3). When the support was α-Al_2O_3 the effect was much less pronounced and on unsupported Pd black the situation was completely different. In the latter case, the ethylene hydrogenation rate decreased slightly when the catalyst was aged. In the presence of carbon monoxide the selectivity was almost constant upon aging even for the supported catalysts. According to Battiston *et al.* (8), who worked under conditions closer to the normal industrial operation with a total pressure of about 20 bar, the selectivity towards ethane increases with aging even when CO is present. The effect is however not nearly as dramatic as when no CO is added

0021-9517/96 $12.00

to the feed. The explanation offered by Sárkány *et al.* (6) for these observations is as follows. The hydrocarbon fragments formed migrate to the support, where they are accumulated. This leaves the metal surface available for acetylene hydrogenation at an almost unchanged rate. The ethylene hydrogenation is believed to take place on the support or on the deposited hydrocarbon residues by means of a hydrogen transfer mechanism, facilitated by the presence of retained oligomers. Carbon monoxide is thought to hinder the spillover of hydrogen from the metal, thereby blocking this route for ethylene hydrogenation.

An alternative explanation, suggested by Schröder (10), is that the accumulation of coke in the pore system leads to an increased intraparticle diffusion resistance. This would result in a lower acetylene partial pressure inside the porous catalyst. The reaction order with respect to acetylene is in the range −0.5–0, so moderate mass transfer limitations are not expected to decrease the acetylene consumption rate. The ethylene hydrogenation rate on the other hand is known to increase dramatically at low acetylene pressures.

The purpose of this study is to investigate to what extent the intraparticle diffusion is influenced by catalyst aging and to find out whether an increased mass transfer resistance is a possible explanation for the unexpected aging behaviour.

METHODS

Apparatus and Procedure

An internal recycle (Berty) reactor from Autoclave Engineers was used in all deactivation runs and reaction rate measurements. Gas composition in the feed and the reactor outlet was analysed with an on-line GC (Varian 3300) equipped with a 25-m Al_2O_3/KCl PLOT column and two detectors (FID + TCD). The gases used were nitrogen 99.996%, ethylene 99.5%, hydrogen 99.98%, and acetylene 99.6%, all supplied by AGA. Trace oxygen and water were removed from the nitrogen gas by means of gas filters. All other gases were used without further purification. Due to the risk of self-explosion acetylene was fed in a premixed gas consisting of acetylene and purified nitrogen. The reactor setup enabled control of reactant partial pressures as well as acetylene conversion, allowing the deactivation runs to be performed at an almost constant gas composition. All deactivation runs were performed at the conditions given in Table 1.

Catalyst Preparation

The catalysts are described in Table 2. Catalysts A and B were prepared by wet impregnation of α-Al_2O_3 and γ-Al_2O_3 pellets (delivered by Süd-Chemie) respectively with $Pd(NO_3)_2$ in 30% HNO_3(aq). After impregnation for 72 h the catalysts were dried at room temperature for 24 h and then at 120°C overnight. The dried samples were calcined in air at 723 K for 3 h. Finally the catalysts were reduced in a mixture of 10% hydrogen in nitrogen and left to cool in flowing nitrogen. Prior to use the catalysts were rereduced in the same mixture at 523 K for 3 h and cooled to the reaction temperature in flowing nitrogen. To isolate the mass transfer effects we used uniformly impregnated catalysts and varied the particle size. To obtain samples with small particles the pellets were crushed and sieved to the desired size interval. Almost spherical particles with a diameter slightly smaller than the original pellet size were obtained by stirring a few grams of catalyst in distilled water for 2 days.

TABLE 1

Reaction Conditions Used in All Deactivation Experiments

Temperature:	308 K		
Total pressure:	1.0×10^6 Pa		
Stirring speed:	3000 rpm		
Catalyst load:	0.3–0.85 g		
Reactor gas composition (mole fractions, balanced by N_2)			
H_2:	0.0115	C_2H_2:	0.0035
C_2H_4:	0.35	$C_2H_6 + C_4^+$:	<0.002

Effective Diffusivity Measurements

The effective pore diffusivity for acetylene was estimated by the method originally proposed by Hougen and Watson (11), that is, by measuring the reaction rate for different particle sizes. The reaction order must of course be known and for the sake of simplicity and accuracy a first-order reaction is preferred. In this case we used the hydrogenation of small amounts of acetylene (<50 ppm) in the presence of 25 ppm CO and a large excess of hydrogen. Under these conditions the intrinsic reaction was close to first order with respect to acetylene. The procedure was to first determine the reaction rate on the full-size catalyst

TABLE 2

Catalyst Properties

Catalyst	A	B	C (Commercial)
Support material	α-Al_2O_3	γ-Al_2O_3	α-Al_2O_3
Pd load (wt%)	0.05	0.056	0.04
Dispersion (moles CO/moles Pd)	0.035	0.041	0.09
BET surface m^2/g)	8	172	—
Pore volume (cm^3/g)	0.23	0.45	
Pd distribution	Uniform	Uniform	Peripheral

particles at a specified acetylene concentration and a few hydrogen levels. The catalyst was then removed from the reactor and crushed carefully to below 0.5 mm. The sample was reloaded into the reactor and the rate was measured again under the same conditions. All samples were stabilized by keeping them at the reaction conditions for 2 h before starting the experiments. The effectiveness factor for the small particles was always close to 1, which is important due to the poorly defined geometry of crushed particles. In a control experiment a sample of deactivated catalyst with a small particle size (0.3–0.4 mm) was exposed to air and/or crushed to very fine particles. It was found that these treatments had a negligible effect on the reaction rate. The effective diffusivity for hydrogen was calculated from the measured value for acetylene, assuming that the diffusivity was inversely proportional to the square root of the molar mass.

Analysis of Coke Content

The accumulated amount of carbonaceous deposits on the spent catalysts was determined by burning off the coke in air at 1023 K. Reference samples, consisting of fresh, reduced catalyst, were treated together with the coked catalyst. The mass of the coke was obtained from the difference in weight loss between the coked samples and the corresponding references. To avoid influence of physisorbed water all samples were dried for at least 48 h in a desiccator before weighing. The change in weight observed for the reference samples was always below 0.1% for Catalyst A, but between 5.2 and 5.4% for Catalyst B due to loss of bonded water. The intraparticle distribution of coke was studied by visual inspection in an optical microscope.

Mass Transfer Modelling

In addition to the experiments, the effects of mass transfer resistance were also investigated by mathematical modelling. All samples of homogeneously impregnated catalysts (A and B) were regarded as spherical, applying an equivalent radius in the case of cylindrical pellets. Eggshell catalysts were treated as semi-infinite slabs with thickness L, assuming that the shell was thin enough to ignore the curvature. Isothermal conditions were assumed in all cases. The intraparticle concentration profiles were obtained from the diffusion equation, written as follows for component i:

$$D_{\text{eff},i}\left(\frac{d^2c_i}{dz^2}+\frac{s}{z}\frac{dc_i}{dz}\right)+\sum_j \nu_{ij}r_j(c)=0. \qquad [1]$$

The geometry parameter s is equal to 2 or 0 in the case of spherical or Cartesian (semi-infinite slab model) coordinates respectively. In the absence of external mass transfer limitations the boundary conditions are

At $z = 0$: $dc/dz = 0$

At $z = d_p/2$ (Eq. [1]): $c_i = c_i^{\text{gas}}$

At $z = L$ (Eq. [2]): $c_i = c_i^{\text{gas}}$.

Due to the reaction conditions used throughout this work (see also the section on kinetic modelling below) the reaction rates could be treated as functions of the acetylene and hydrogen partial pressures only. It was therefore sufficient to consider only the concentration profiles of these two components. The solution to Eq. [1] was computed numerically using orthogonal collocation.

RESULTS

Reactor Verification

The recycle reactor was checked for nonidealities according to the procedures described by Bos *et al.* (12) and Georgakopoulos and Broucek (13). The recirculation ratio was always larger than 130 and the reactor could safely be regarded as perfectly mixed. The absence of film transfer limitations was carefully verified through measurements of the gas–solid temperature difference, variation of the stirring speed, and estimation of transfer coefficients (14).

Kinetic Modelling

To understand the effects of mass transfer limitations one must start with the kinetics of the surface reaction. Here only the rate dependence on acetylene and hydrogen partial pressures are considered, since all deactivation runs were performed at constant temperature and in the absence of CO. The following overall reaction scheme was assumed for the purpose of rate modelling:

1. $C_2H_2 + H_2 \rightarrow C_2H_4$
2. $C_2H_4 + H_2 \rightarrow C_2H_6$
3. $2C_2H_2 + H_2 \rightarrow C_4H_6$
4. $2C_2H_2 + 2H_2 \rightarrow C_4H_8$

It has been shown by Margitfalvi *et al.* (15) that the formation of ethane directly from acetylene is negligibly small compared to the ethylene hydrogenation, so this reaction was omitted. A separate experiment showed that the rate of butene formation was independent of the partial pressure of butadiene + butyne, and it was therefore assumed that all the butene was formed from acetylene and hydrogen. The above reactions accounted for more than 95% of the total acetylene consumption. The remaining part,

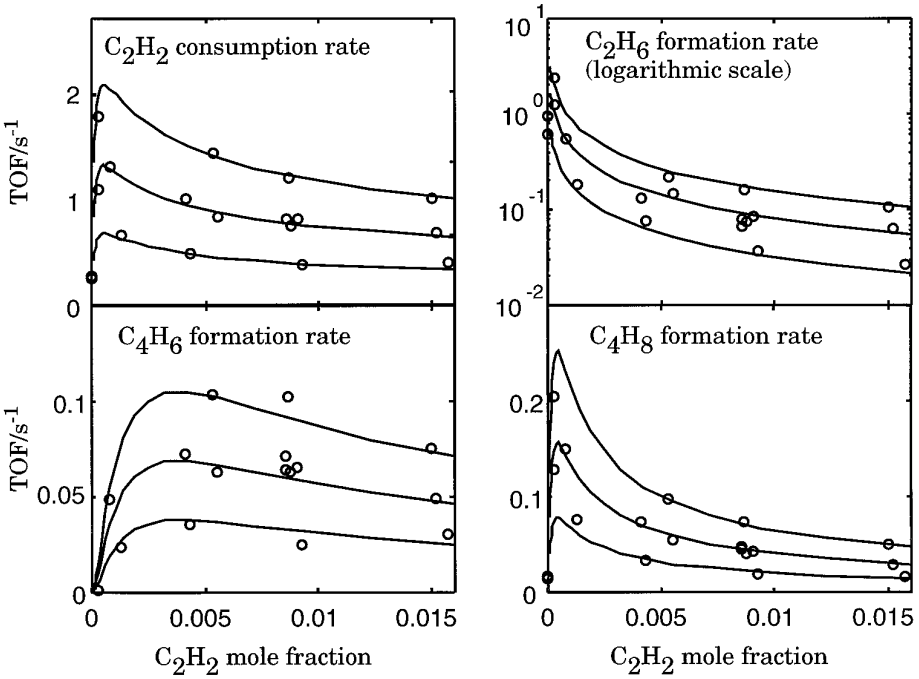

FIG. 1. Results from experiments to investigate reaction kinetics. Observed (circles) and modelled (lines) reaction rates. The three lines in each graph represents different levels in hydrogen pressure. Experimental conditions are given in the Appendix.

which was neglected here, was mainly due to the formation of higher hydrocarbons, some of which were retained on the catalyst.

The experimental results are plotted in Fig. 1 together with the model predictions, while the models and experimental conditions are given in the Appendix. The rate expressions used are essentially empirical and selected on the basis of good fit. All experiments concerning reaction kinetics were performed using fresh Catalyst A. Control experiments showed that the commercial Catalyst C behaved very similarly. Catalyst B on the other hand showed very rapid initial coke formation and a significantly higher ethane formation, making the model insufficient for this catalyst.

As a first observation note that the reaction order with respect to acetylene is negative except for very low partial pressures. Moreover, the ethylene hydrogenation rate increases dramatically as the acetylene pressure approaches zero.

Catalyst Deactivation

For the discussion of the deactivation results it is convenient to define measures of activity and product distribution. The catalyst activity is measured by the turnover frequency (TOF) for acetylene hydrogenation defined as

$$\mathrm{TOF} = \frac{\text{Rate of } C_2H_2 \text{ consumption } (s^{-1})}{\text{Nr of exposed Pd sites on a fresh catalyst}}.$$

The product distribution is characterised by three different selectivities:

$$S_{26} = \frac{\text{molar rate of } C_2H_6 \text{ formation}}{\text{molar rate of } C_2H_2 \text{ consumption}}$$

$$S_{46} = 2 \times \frac{\text{molar rate of } C_4H_6 \text{ formation}}{\text{molar rate of } C_2H_2 \text{ consumption}}$$

$$S_{48} = 2 \times \frac{\text{molar rate of } C_4H_8 \text{ formation}}{\text{molar rate of } C_2H_2 \text{ consumption}}.$$

The objective of this process when run commercially is to remove all but a few parts per million of the acetylene, preferably by converting it to ethylene. Consequently, all the selectivities defined above represent unwanted side reactions and it is advantageous to keep them as small as possible.

The results from deactivation runs using Catalyst A with different particle sizes are presented in Fig. 2. The catalyst performance during the first hours on stream is independent of the particle size, showing that mass transfer effects have no influence on the reactions. After a certain time on stream the product distribution changes markedly except when the smallest particles are used. In this case all reaction rates are almost completely stable during at least 100 h.

After about 115 h on stream the 3-mm pellets were removed from the reactor and crushed to below 0.5 mm.

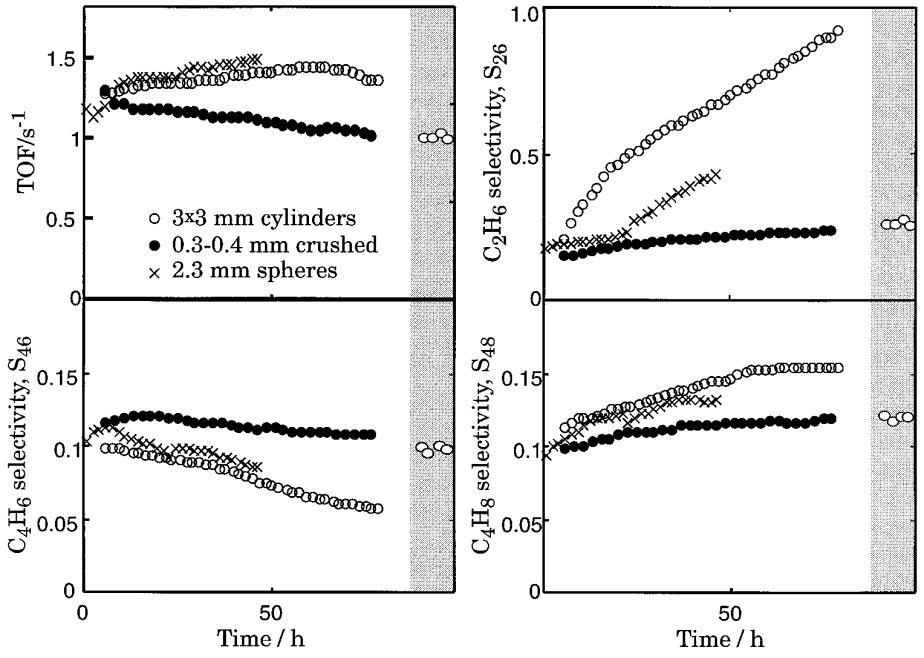

FIG. 2. Activity and product distribution obtained during aging of Catalyst A (Pd/α-Al_2O_3). The points in the shaded area show the performance of the deactivated 3.0-mm pellets after crushing to below 0.5 mm.

The catalyst was then put back into the reactor and the reaction mixture was fed directly, without any pretreatment. As seen in Fig. 2 the catalyst performance almost completely recovered by the reduction of the particle size. When the catalyst was not crushed, exposure to air for 72 h had no effect on the catalyst performance.

The effective pore diffusivities of the fresh and deactivated catalyst were measured by the Hougen–Watson method described above with the experimental results given in Table 3. Aging the catalyst for about 115 h caused a decrease in the apparent pore diffusivity by nearly a factor of 10.

TABLE 3

Properties of Deactivated Catalysts

Catalyst	Particle size (mm)	Time on stream (hours)	Coke, C_c (wt%)	$10^7 \times D_{eff}$ (m^2/s)
A	3 × 3 (cyl)	0	0	3.6
A	3 × 3 (cyl)	24	3.0	1.1
A	0.3–0.4 (crush.)	24	4.1	—
A	~2.3 (spheres)	48	4.9	0.63
A	3 × 3 (cyl)	65	5.0	0.59
A	3 × 3 (cyl)	115	10.2	0.32
A	3 × 3 (cyl)	120	9.3	0.35
A	0.3–0.4 (crush.)	72	9.7	—
B	4.2 × 4.2 (cyl)	0	0	3.3
B	~3.0 (spheres)	22	13.4	1.9
B	1.5–1.8 (crush.)	22	19.7	—
B	1.5–1.8 (crush)	48	22.8	0.66
C	3.5 × 3.5	28	3.65	—

The effect of increased mass transfer resistance was also calculated from the mass transfer model described above, assuming that the intrinsic reaction rates are unaffected by the coke laydown. Calculation results concerning Catalyst A (pellets) are presented in Fig. 3 together with the experimental observations. Note that the predictions in the figure are not fitted to the experimental data but calculated using Eq. [1] and the rate equations in the Appendix. The general agreement is remarkably good for all considered reactions, and all the trends observed are accounted for by the model.

Deactivation experiments of the same type were also performed with Catalysts B to investigate the influence of the support. As with Catalyst A, there was no influence of particle size when fresh samples were used. On the other hand, as seen in Fig. 4, when the catalyst was aged mass transfer effects became pronounced with respect to selectivity. On Catalyst B the ethane selectivity was generally higher than on Catalyst A, and the ethane formation also increased significantly during the first 20–25 h even for very small particles. The coke formation was much more rapid than on Catalyst A (see Table 3) with the average carbon laydown during the first 24 h corresponding to up to 20% of the total acetylene consumption. The deactivation was replicated with ethylene removed from the feed, making it possible to obtain the coking rate with good accuracy from an acetylene mass balance. It was then possi-

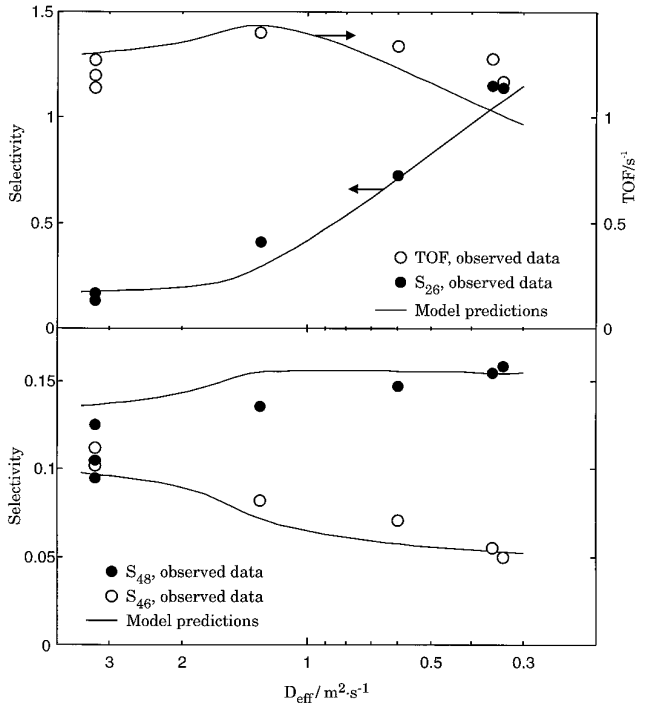

FIG. 3. Observed and calculated performance of fresh and deactivated samples of Catalyst A. Note that the x axis has been reversed, so the diffusivity decreases from left to right. This means that the age of the catalysts used to obtain the experimental points increases from left to right.

ble to calculate a coke selectivity S_c, defined as the fraction of consumed acetylene that could not be accounted for by volatile reaction products. Figure 5 shows the TOF, S_{26}, and the coke selectivity observed in such an experiment. The coke formation is fast, and particularly in the beginning of the run it contributes significantly to the total acetylene consumption.

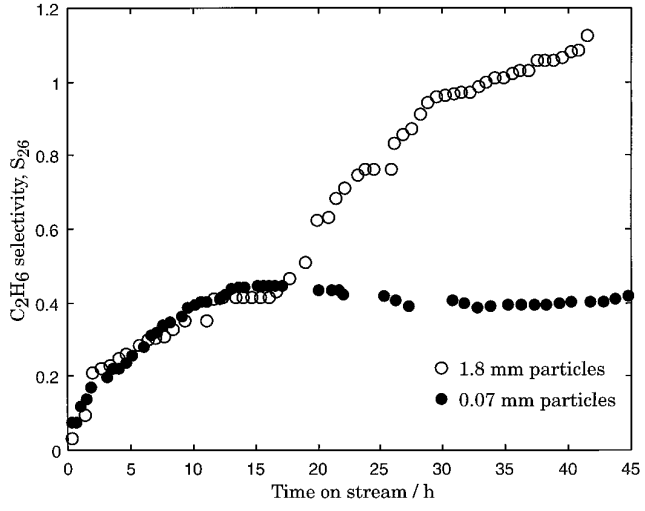

FIG. 4. Ethane selectivity, S_{26}, obtained with deactivating samples of Catalyst B (Pd on γ-Al_2O_3).

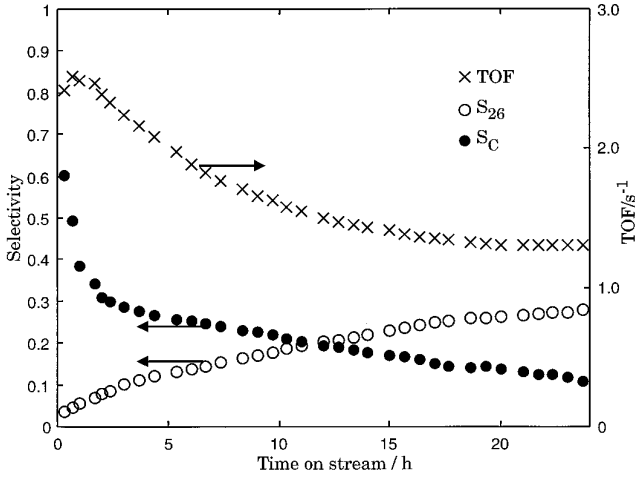

FIG. 5. Acetylene consumption, TOF, ethane selectivity, S_{26}, and coke selectivity, S_c, obtained on Catalyst B (Pd/γ-Al_2O_3) with no ethylene present in the feed. Note the high acetylene consumption due to coke formation, especially during the first hours.

The coke formation on pure support was investigated in a set of experiments summarized in Table 4. The support samples were given the same treatment (calcination, reduction) as Catalysts A and B (see above) and the experimental conditions were the same as in all other deactivation runs (Table 1). When the reactor was loaded with pure support only, no measurable reactions or coke formation took place. When a Pd catalyst was also present in the reactor, the coke formation became substantial on γ-Al_2O_3 but there was still no deposition on pure α-Al_2O_3.

Commercial catalysts as well as the ones used by many other researchers are normally of the eggshell type making the diffusion limitations less important. It is therefore important to investigate if the mass transfer phenomena described above could be important even in case of shell catalysts. The matter was investigated by means of simulations and experiments using the commercial Catalyst C. In the calculations the thickness of the active shell was

TABLE 4

Investigation of Coke Formation on Pure Support Materials

Support and catalyst	Time on stream (h)	Coke (wt%)
α-Al_2O_3 only	110	<0.05
α-Al_2O_3 + Catalyst A	120	<0.05
γ-Al_2O_3 only	110	0.8
γ-Al_2O_3 + Catalyst A	120	7.5

Note. In the experiments where Catalyst A was loaded it was separated from the pure support particles by a layer of glass beads.

TABLE 5

Conditions Used in the Simulation of the Performance of an Eggshell Catalyst

Process conditions: see Table 1	
	Catalyst data
Metal load:	0.05 wt% (Based on the whole catalyst particles. The local metal concentration in the active shell will be higher and vary with the depth of the active layer.)
Pd dispersion:	0.10
Pellet size:	3.5 mm (spherical)
D_{eff}	0.35×10^{-7} m^2/s (From Table 3, on deactivated catalyst A.)

varied while all other conditions were kept constant as presented in Table 5. The model equations can be found above and the reaction kinetics were assumed to be the same as those on Catalyst A (see Appendix). Figure 6 shows the results of these calculations in terms of rate and ethane selectivity. Evidently, pore diffusion can have a considerable effect even with eggshell catalysts. Experimental results are given in Fig. 7. The catalyst is clearly more stable to aging when crushed to a very small particle size.

Intraparticle Coke Profiles

Optical micrographs of typical coke profiles obtained with different catalysts are shown in Fig. 8. On Catalyst C the coke is almost exclusively deposited in the thin Pd-containing shell near the particle surface showing that the coke formation takes place mainly on the metal. Even on the uniformly impregnated Catalysts A and B the coke deposition is concentrated towards the pellet periphery. A comparison with the fresh sample shows, however, that at least on Catalyst A, there is a considerable amount of coke even in the interior of the particles. On the Pd/γ-Al_2O_3 Catalyst B the coke forms a well-defined shell that appears to be growing towards the pellet centre. When the catalyst had been used for 48 h it had a uniform, almost completely black colour.

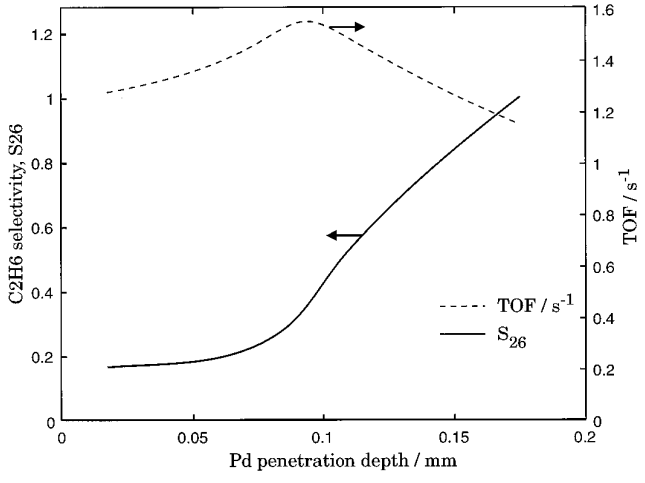

FIG. 6. Simulation results showing the expected performance of a typical commercial eggshell catalyst as a function of the depth of the active shell. Operating conditions and catalyst properties are given in Table 5.

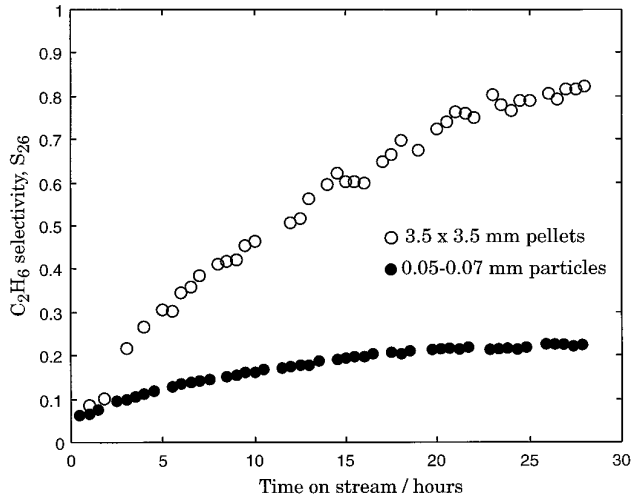

FIG. 7. Ethane selectivity obtained with crushed and noncrushed samples of the commercial shell-type Catalyst C.

DISCUSSION

The results obtained with all catalysts show one dominating effect of deactivation: The rapid formation of large amounts of polymers or coke that fill up the pore system and cause a significant decrease in the effective diffusivity. The apparently complicated influence on the product distribution arises as a combined effect of mass transfer limitations and the complex kinetics. The acetylene consumption rate obtained on large catalyst particles exhibits a maximum after about 50 h (Fig. 2). This is an expected effect of an increased diffusion resistance considering the negative reaction order with respect to acetylene and the positive order with respect to hydrogen. The same trends are predicted by the model calculations presented in Figs. 3 and 6.

Judging from the experiments with small catalyst particles (Fig. 2), the intrinsic reaction rates on Catalyst A (Pd on α-Al_2O_3) are almost unaffected by the coke laydown, at least up to a coke concentration of about 10% (w/w). This conclusion is further supported by the calculations presented in Fig. 3. The effect of coke deposition on all considered reactions can obviously be predicted by a model that accounts for mass transfer effects only. Previous authors (6, 16) have suggested that the coke, although formed on the metal, accumulates primarily on the support, leaving

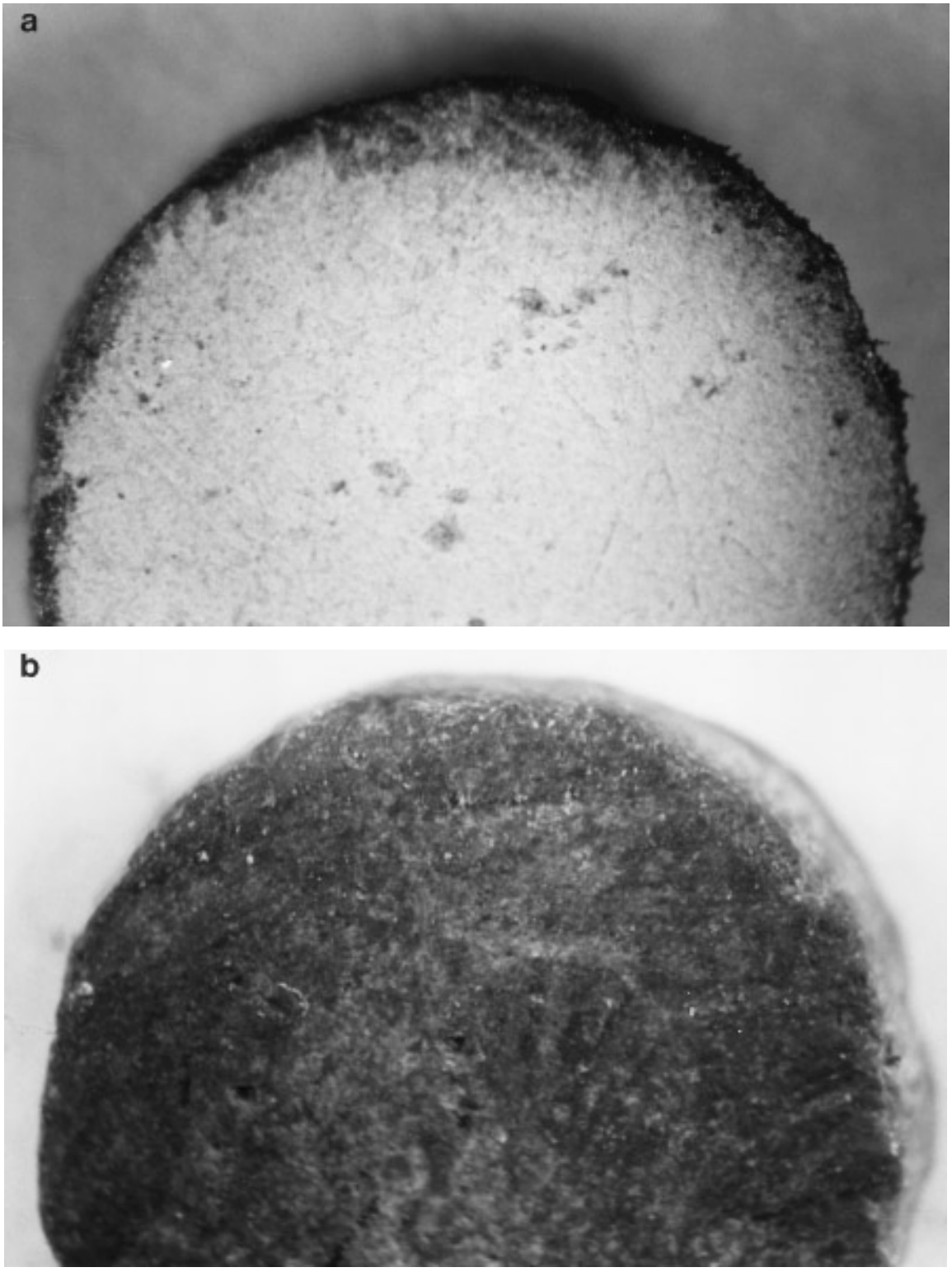

FIG. 8. Optical micrographs showing the intraparticle coke distribution. Magnification: 40×. (a) Cross section of Catalyst A(Pd/α-Al_2O_3) used 120 h. (b) Outer surface of Catalyst A used 120 h. (c) Cross section of Catalyst B (Pd/γ-Al_2O_3) used 22 h. (d) Cross section of Catalyst C (commercial shell-type Pd/α-Al_2O_3), used 28 h.

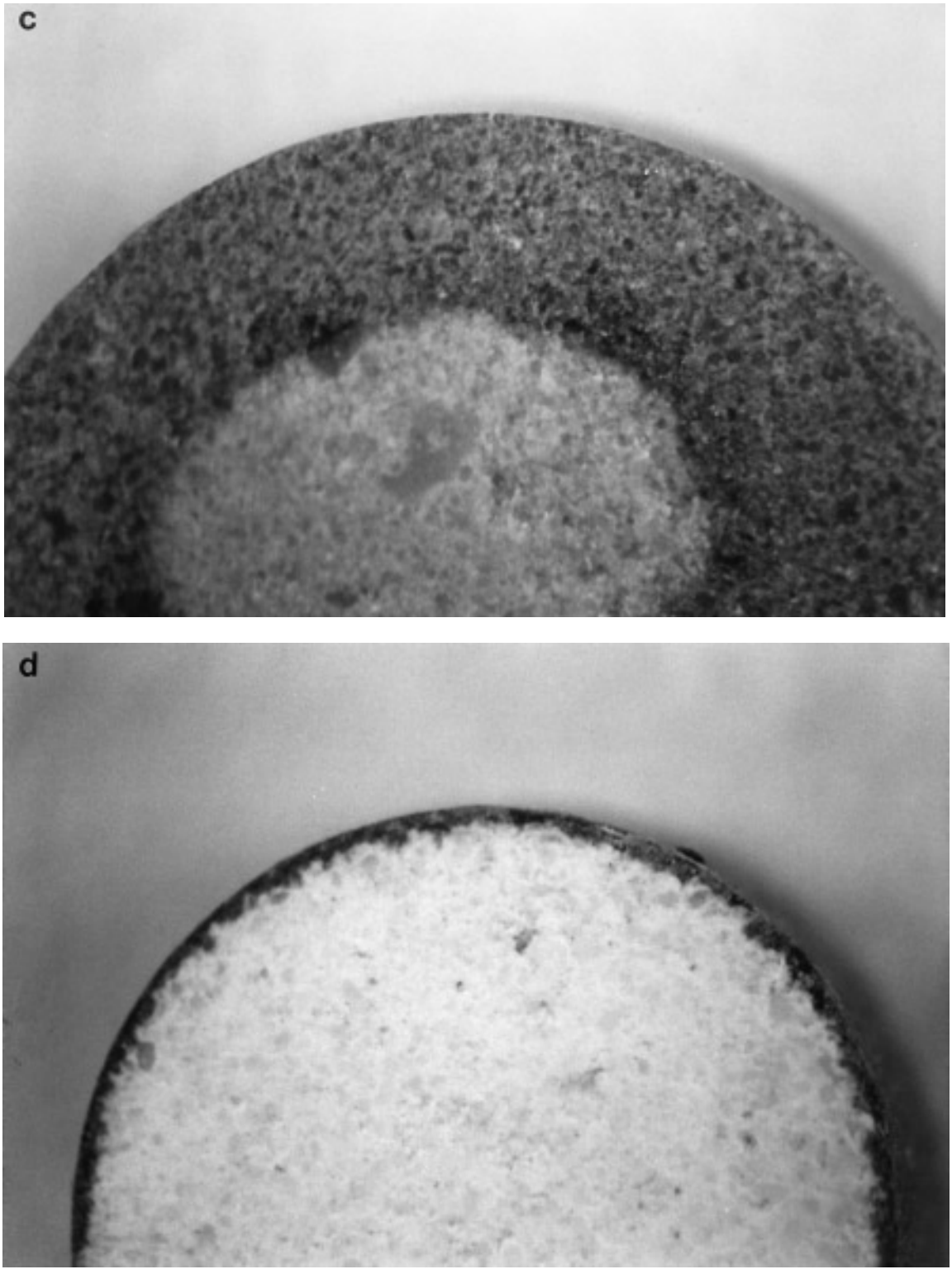

Fig. 8—*Continued*

the Pd surface free for reaction at an almost unchanged intrinsic rate.

When γ-Al_2O_3 is used as the support (Catalyst B), the ethane selectivity increases independently of the particle size during the first 15–20 h. This indicates a change in the intrinsic rate of ethylene hydrogenation and may support the explanation offered by Sárkány *et al.* (6). Ethylene is supposed to react on the surface of the support by means of a hydrogen transfer mechanism involving the deposited coke. The rate of this reaction is expected to be much lower on Catalyst A due to the lower BET surface area and chemical activity of the support.

An important effect, not considered in (6), is that the relatively low initial ethane selectivity seen in Fig. 4 is in part caused by the rapid coke formation. The coking reactions cause significant acetylene consumption, particularly during the first hours, which is not due to the main reaction scheme. It can be deduced from Fig. 5 that the coke selectivity is not high enough to fully explain the observed selectivity change, but it does have a considerable influence on the results. The coke formation in the work by Sárkány *et al.* (6) was claimed to correspond to about 2% of all the consumed acetylene and it was therefore neglected in the selectivity calculations. However, from their given data it can be calculated that on a Pd/γ-Al_2O_3 catalyst the retained species formed during the first 50 h of operation correspond to more than 40% of the acetylene consumption. This is obviously not negligible and without knowledge of the coke selectivity variation with time it is difficult to interpret the results in (6) correctly.

The relation between coke formation and intraparticle diffusion has been studied previously for single-reaction systems (17–19). A theoretical investigation was recently published by Lee (20), who has derived the following equation for the local effective diffusivity as a function of the coke content:

$$\frac{D_{\text{eff}}}{D^0_{\text{eff}}} = \left(1 - \frac{C_c}{C^s_c}\right)^{\beta}, \qquad [2]$$

where D^o_{eff} is the effective diffusivity of the fresh catalyst and C^s_c is the coke concentration required to fill the entire pore volume. The parameter β can be calculated from random-pore models to be 1 (model of Feng and Stewart (21)) or 2 (model of Wakao and Smith (22)). In this case we have measured the global diffusivity and Eq. [2] will hold only if the coke formation is uniform inside the catalyst particles. As seen in the micrographs of Fig. 8 the coke deposition on Catalyst A is not uniform but concentrated towards the pellet surface. This type of coke profile will result in the formation of a layer of high diffusion resistance and the global diffusivity will therefore appear to be low

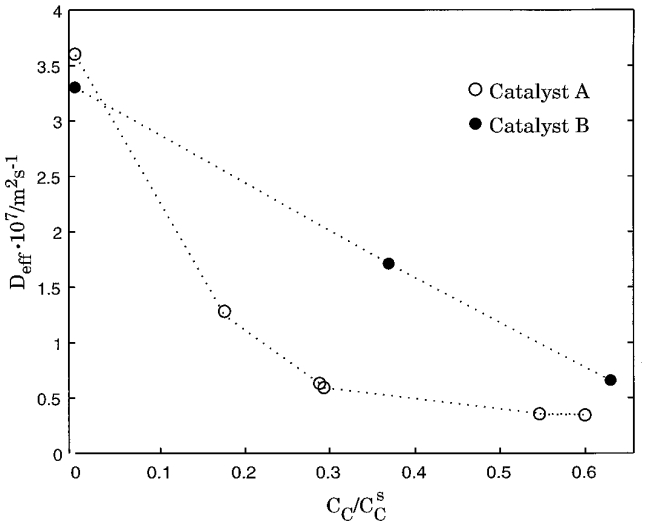

FIG. 9. Measured effective diffusivities for acetylene in deactivated catalysts versus extent of coking. The coke concentration at saturation, C^s_C, have been determined from pore volume measurements on coked catalysts to: Catalyst A, C^s_C = 17 wt%; Catalyst B, C^s_C = 36 wt%.

even if the average coke concentration is moderate. In Fig. 9 it can be seen that this is the behaviour exhibited by Catalyst A. From the data given in (8), the coking reaction order with respect to acetylene can be estimated to be between 1.5 and 2 at a constant hydrogen pressure. The intraparticle gradient in acetylene partial pressure will therefore have a strong influence on coke formation, explaining the nonuniform deposition.

The rate of coke deposition was much higher on Catalyst B than on Catalyst A (Table 3) although the Pd load and dispersion are very similar. The difference in the coking rate and intraparticle coke profiles (Fig. 8) must therefore be attributed to the support. The α-alumina support of Catalyst A is inactive for coke formation (Table 4). The γ-alumina used in Catalyst B, on the other hand, has a larger internal area and is active for coke deposition, but only if the reactor is also loaded with impregnated catalyst (Table 4). The results suggest that the coke deposition proceeds via a precursor, which is formed on the metal surface. Battiston *et al.* (8) have found that no surface polymers are formed in the absence of hydrogen even on Pd-impregnated catalysts. It is therefore reasonable to conclude that partial hydrogenation is a required step in the formation of the main coke precursor. These data are clearly not sufficient to identify the precursor, but butadiene and larger conjugated dienes are probable candidates. These compounds polymerise readily to give coke (23, 24) and are formed during acetylene hydrogenation.

The coke profile inside the used particles of Catalyst B exhibits a very sharp front (Fig. 8c). A possible explanation

is that the initial coke formation occurs through addition of monomers to growing surface polymer chains (25). The chain propagation reaction proceeds through a carbonium ion mechanism and is catalysed by acidic sites on the clean γ-alumina support. The effect is the formation of a coke monolayer, growing at the edge and maintaining a sharp front until the whole support surface is covered.

The intraparticle mass transfer was found to have a pronounced influence even on an eggshell catalyst (Fig. 7). The Pd-containing outer shell of Catalyst C was estimated to be 80–100 μm deep by inspection of a fresh, reduced pellet in an optical microscope. As a comparison, Wright *et al.* (26) used a proton-induced X-ray technique and found the Pd layer of an unspecified commercial catalyst for acetylene hydrogenation to be about 200 μm. It is clear from Fig. 6 that these values are within the range where mass transfer limitations might be important. The rapid aging of Catalyst C (Fig. 7) can be explained by the high metal concentration in the active shell. In addition, the pore volume of the active part of the catalyst is small and can be completely filled with only a small amount of coke. As an example, 3.65 wt% as was deposited on Catalyst C in 28 h, is enough to fill the entire pore system in the outer 80 μm of the pellets (assuming a coke density of 1000 kg/m^3).

The mass transfer effects observed in this study can be expected to be important also in full-scale processes, where coke concentrations of at least 20% (w/w) have been reported (8). The effects of concentration gradients will however be different in the presence of carbon monoxide, which is usually used industrially. According to McGown *et al.* (27) and the rate equation given in (12), the reaction order with respect to acetylene in this case varies between 0 and 1. Further, the ethane formation is not as sensitive to low acetylene levels when CO is present. This means that the expected effect of coke-induced mass transfer limitations is a decreased acetylene consumption rate and moderately increased ethane selectivity. It is interesting that Battiston *et al.* (8), using a micropilot plant under industrial conditions, found exactly that aging behaviour.

CONCLUSIONS

Supported Pd catalysts used in the selective hydrogenation of acetylene are subject to aging due to the deposition of polymeric hydrocarbons referred to as coke or green oil. These retained species cause a significantly increased resistance to intraparticle diffusion, which in turn has a detrimental effect on the selectivity to ethylene. The effect can be pronounced even for eggshell catalysts.

The choice of support is critical for the catalyst performance. α-Al_2O_3 is preferred in comparison to γ-Al_2O_3 as the latter increases the coke formation and the undesired ethane formation. The intrinsic ethane formation rate also increases with deactivation when the support is γ-Al_2O_3.

A conclusion with implications for experimental work is that when coke formation occurs, it is not sufficient to verify the absence of mass transfer limitations on a fresh catalyst. The effective diffusivity can decrease by at least an order of magnitude, creating a limitation that is not detectable on a new catalyst.

APPENDIX: EMPIRICAL RATE EQUATIONS

The kinetic equations used for mass transfer calculations describe all reaction rates on Catalyst A (Pd on α-Al_2O_3) as a function of the acetylene and hydrogen partial pressures only. The experimental conditions used to obtain the parameters were:

Temperature:	308 K	H_2 mole fraction:	0.007–0.018
Total pressure:	10 bar	C_2H_2 mole fraction:	2×10^{-5}–0.02
C_2H_4 mole fraction:	0.3		
Catalyst particle size:	0.25–0.4 mm		

Each catalyst sample was operated for a maximum of 16 h, during which time no deactivation was observed. Prior to the first measurement after loading a fresh catalyst sample, the gas composition was kept constant for about 4 h to ensure stable activity.

The rate equations used were

$$r_1 = k_1 \frac{p_{C_2H_2} p_{H_2}^{b_1}}{(1 + K p_{C_2H_2})^{a_1}}, \quad r_2 = k_2 \frac{p_{H_2}^{b_2}}{(1 + K p_{C_2H_2})^{a_2}}$$

$$r_3 = k_3 \frac{p_{C_2H_2}^2 p_{H_2}^{b_3}}{(1 + K_3 p_{C_2H_2})^{a_3}}, \quad r_4 = k_4 \frac{p_{C_2H_2}^2 p_{H_2}^{b_4}}{(1 + K p_{C_2H_2})^{a_4}},$$

where p_i is the partial pressure of component i normalized by a standard pressure of 10^5 Pa.

Note that the ethylene hydrogenation rate is written as independent of the ethylene pressure. This is due to the fact that the ethylene pressure was kept constant in all the experiments. In principle, a term corresponding to the coverage of ethylene could be included in the denominator of the equations above. However, since the ethylene pressure was constant this term is unnecessary in the present

case, but it should be noted that the parameter K cannot be interpreted as an adsorption equilibrium constant.

The final parameters as determined from nonlinear regression where

$k_1 = 2.30 \times 10^4$	molecules (site · s)
$k_2 = 0.99 \times 10^2$	molecules (site · s)
$k_3 = 1.56 \times 10^4$	molecules (site · s)
$k_4 = 3.55 \times 10^6$	molecules (site · s)
$K = 472.1$	$K_3 = 84.0$
$a_1 = 1.45$	$b_1 = 1.16$
$a_2 = 1.02$	$b_2 = 1.61$
$a_3 = 2.66$	$b_3 = 1.04$
$a_4 = 2.87$	$b_4 = 1.36$

ACKNOWLEDGMENTS

NUTEK is gratefully acknowledged for financial support. The author also thanks Jan Karlsson for valuable assistance in preparing the optical micrographs.

REFERENCES

1. Derrien, M. L., *Stud. Surf. Sci. Catal.* **27,** 613 (1986).
2. Bos, A. N. R., and Westerterp, K. R., *Chem. Eng. Process.* **32,** 1 (1993).
3. Park, Y. H., and Price, G. L., *Ind. Eng. Chem. Res.* **30,** 1693 (1991).
4. Cider, L., and Schöön, N.-H., *Ind. Eng. Chem. Res.* **30,** 1437 (1991).
5. Schröder, U., and Schöön, N-H., *J. Catal.* **143,** 381 (1993).
6. Sárkány, A., Guczi, L., and Weiss, A. H., *Appl. Catal.* **10,** 369 (1984).
7. Weiss, A. H., Gambhir, B. S., LaPierre, R. B., and Bell, W. K., *Ind. Eng. Chem. Proc. Des. Dev.* **16,** 352 (1977).
8. Battiston, G. C., Dalloro, L., and Tauszik, G. R. *Appl. Catal.* **2,** 1 (1982).
9. Asplund, S., Fornell, C., Holmgren, A., and Irandoust, S., *Catal. Today* **24,** 181 (1995).
10. Schröder, U., "Carbon Monoxide in Catalytic Hydrogenation, A Poison or a Promoter?," Ph.D. thesis, Chalmers University of Technology, Göteborg, Sweden, 1993.
11. Hougen, O. A., and Watson, K. M., "Chemical Process Principles, Part III, Kinetics and Catalysis." Wiley, London, 1947.
12. Bos, A. N. R., Bootsma, E. S., Foeth, F., Sleyster, H. W. J., and Westerterp, K. R., *Chem. Eng. Process.* **32,** 53 (1993).
13. Georgakopoulos K., and Broucek, R., *Chem. Eng. Sci.* **42,** 2782 (1987).
14. Yoshida, F., Ramaswami, D., and Hougen, O. A., *AIChE J.* **8,** 5 (1962).
15. Margitfalvi J., Guczi L., and Weiss, A. H., *J. Catal.* **72,** 185 (1981).
16. LeViness, S., Nair, V., and Weiss, A. H., *J. Mol. Catal.* **25,** 131 (1984).
17. Butt, J. B., Delgado-Diaz, S., and Muno, W. E., *J. Catal.* **37,** 158 (1975).
18. Ozawa, Y., and Bischoff, K. B., *Ind. Eng. Proc. Des. Dev.* **7,** 67 (1968).
19. Suga, K., Morita, Y., Kunugita, E., and Otake, T., *Int. Chem. Eng.* **7,** 742 (1967).
20. Lee, H. H., *AIChE J.* **40,** 2022 (1994).
21. Feng, C. F., and Stewart, W. E., *Ind. Eng. Chem. Fund.* **12,** 143 (1973).
22. Wakao, N., and Smith, J. M., *Ind. Eng. Chem. Fund.* **3,** 123 (1964).
23. Lin, T.-B., and Chou, T.-C., *Appl. Catal.* **108,** 7 (1994).
24. Parera, J. M., Verderone, R. J., and Querini, C. A., *in* "Catalyst Deactivation 1987" (B. Delmon and G. F. Froment, Eds.). Elsevier, Amsterdam, 1987.
25. Trimm, D. L., *Appl. Catal.* **5,** 263 (1983).
26. Wright, J., McMillan, J. W., and Cookson, J. A., *J. Chem. Soc. Chem. Commun.,* 968 (1979).
27. McGown, W. T., Kemball, C., and Whan, D. A., *J. Catal.* **51,** 173 (1978).